CROATICA CHEMICA ACTA
CCACAA **80** (3-4) 517–527 (2007)
ISSN-0011-1643
CCA-3194
Original Scientific Paper

Formation of Magnetite in Highly Alkaline Media in the Presence of Small Amounts of Ruthenium*

Stjepko Krehula and Svetozar Musić**

Division of Materials Chemistry, Ruđer Bošković Institute, P.O. Box 180, HR-10002 Zagreb, Croatia

RECEIVED DECEMBER 5, 2006; REVISED APRIL 3, 2007; ACCEPTED APRIL 5, 2007

The effect of small amounts of ruthenium on the formation of magnetite in highly alkaline media was investigated using X-ray powder diffraction (XRD), Mössbauer and FT-IR spectroscopies, field emission scanning electron microscopy (FE-SEM) and energy dispersive X-ray spectroscopy (EDS). Acicular α-FeOOH particles precipitated in a highly alkaline medium with the addition of tetramethylammonium hydroxide (TMAH) were used as a reference material. Initial addition of small amounts of $Ru(NO)(NO_3)_3$ to that precipitation system had a drastic effect on the formation of iron oxide phases and their properties. The addition of $Ru(NO)(NO_3)_3$ favoured the formation of stoichiometric Fe_3O_4. With an increase of the initial $Ru(NO)(NO_3)_3$ concentration in the precipitation systems less time was needed for the formation of Fe_3O_4 as a single Fe-bearing phase in the precipitates. Ruthenium ions made solid solutions α-(Fe,Ru)OOH; however, there was no indication of the formation of solid solutions with α-Fe_2O_3 and Fe_3O_4. Mössbauer and FT-IR spectroscopies supported the conclusion on the formation of solid solutions α-(Fe,Ru)OOH. FE-SEM showed the formation of octahedral Fe_3O_4 particles of a μm range size. Ruthenium particles (≈ 20 nm in size) were deposited onto the surfaces of Fe_3O_4 particles. They were also present in the form of clusters containing octahedral Fe_3O_4 particles in the nanosize range (≈ 100 nm or less). The formation of Fe_3O_4 was interpreted as a combining effect of the thermal decomposition products of TMAH under autoclaving conditions and the catalytic action of ruthenium. In such a way strong reductive conditions in the investigated precipitation system were created.

Keywords
ruthenium
TMAH
magnetite
XRD
Mössbauer
FT-IR
FE-SEM
EDS

INTRODUCTION

Magnetite (Fe_3O_4) shows unique magnetic and electrical properties and due to that it has been the subject of many investigations. Verwey and De Boer[1] solved the crystal structure of magnetite and Fleet[2,3] further refined it. Magnetite has the inverse-spinel structure with space group *Fd3m* and lattice constant a = 8.394(5) Å.[4] Fleet[2] measured a = 8.3941(7) Å for natural magnetite. Iron ions occupy two distinct structural positions in magnetite: Fe^{3+} ions are at tetrahedral sites, whereas Fe^{2+} and Fe^{3+} ions are equally distributed at octahedral sites of the spinel-type structure. Fe_3O_4 undergoes a sharp phase transition at near ≈ 120 K,[5] which phenomenon is often cited in reference literature as the Verwey transition. This transition is related to an abrupt decrease in electric conductivity and a specific heat anomaly. ^{57}Fe Mössbauer spectrum of Fe_3O_4 is characterized by two hyperfine magnetic fields (two sextets) at room temperature (RT). In the region of

* Dedicated to Professor Nikola Kallay on the occasion of his 65th birthday.

** Author to whom correspondence should be addressed. (E-mail: krehul@irb.hr)

TABLE I. Conditions for the preparation of the samples by autoclaving at 160 °C (total volume of the each precipitation system is 40 mL)

Sample	$[FeCl_3]$ / mol dm^{-3}	$[Ru(NO)(NO_3)_3]$ / mol dm^{-3}	$r = [Ru] / ([Ru] + [Fe])$	Volume 25 % *w* TMAH / mL	Autoclaving time / hours
G	0.1	0	0	10	2
G1	0.1	0	0	10	72
R1	0.1	1.0×10^{-5}	1.0×10^{-4}	10	72
R2	0.1	2.5×10^{-5}	2.5×10^{-4}	10	24
R3	0.1	1.0×10^{-4}	1.0×10^{-3}	10	24
R4	0.1	2.5×10^{-4}	2.5×10^{-3}	10	2
R5	0.1	2.5×10^{-4}	2.5×10^{-3}	10	24
R6	0.1	5.0×10^{-4}	5.0×10^{-3}	10	2
R7	0.1	5.0×10^{-4}	5.0×10^{-3}	10	24

Verwey transition and temperatures below it, the Mössbauer spectrum starts to be very complicated. Hargrove and Kündig[6] reported more than two sextets present in the region of Verwey transition, and later investigations[7–10] confirmed this finding. Moreover, the Mössbauer spectrum of Fe_3O_4 was interpreted as the superposition of several sextets. However, there are still uncertainties about the origin of these sextets.

Synthetic magnetite is a very important material in various applications where its chemical or magnetic properties are exploited. Fe_3O_4 and substoichiometric $Fe_{3-x}O_4$ are the typical products of iron (steel) rusting under different conditions.[11,12] Magnetite can be prepared in the laboratory using different synthesis methods. The common way to prepare Fe_3O_4 particles is the oxidation of an aqueous $Fe(OH)_2$ suspension precipitated from Fe^{II}-salt solutions.[13,14] Magnetite can be obtained by adding alkali to the aqueous solutions of Fe^{II}/Fe^{III}-salts.[15] The phase composition of thus obtained precipitates depends on the pH and temperature. Magnetite particles were also formed by a reaction of ferric oxyhydroxides with ferrous species,[16,17] or by the reduction of hematite in a H_2 stream at higher temperature, with the retention of the original hematite particle shape.[18] Thermal decomposition of iron--organic salts is a very simple method for the preparation of magnetite.[19] On the other hand, the disadvantages of this method are a difficult control of the size and morphology of the particles and the presence of additional unwanted phases such as maghemite (γ-Fe_2O_3) and hematite (α-Fe_2O_3). A similar situation occurs in the pyrolysis of aerosol droplets containing an Fe-bearing component, where additional phases, γ-Fe_2O_3 and α-Fe_2O_3, can also be formed. Very small magnetite particles can be obtained by combining the microemulsion method with γ-irradiation.[20] The product of these syntheses methods is usually substoichiometric magnetite ($Fe_{3-x}O_4$). Recently, Krehula and Musić[21] have found that stoichiometric magnetite can precipitate in alkaline aqueous media when ruthenium ions are present. In this work we have extended our investigations to much lower concentrations of ruthenium ions than those used in the previous work,[21] with an aim to obtain more data about that precipitation system, as well as about the corresponding precipitation mechanism.

EXPERIMENTAL

Preparation of Samples

Analytical reagents $FeCl_3 \cdot 6H_2O$ and $Ru(NO)(NO_3)_3$ were used. Tetramethylammonium hydroxide solution (25 %, mass fraction, *w*, electronic grade 99.9999 %) supplied by *Alfa Aesar* was used. Twice-distilled water prepared in our own laboratory was used in all experiments. The experimental conditions for the preparation of G- and R-samples are given in Table I. In the preparation of R-samples a predetermined volume of the TMAH solution (10 mL) was added to the mixed $FeCl_3$ + $Ru(NO)(NO_3)_3$ solutions. The total volume of each precipitation system was 40 mL. The suspensions so formed were vigorously shaken for approximately 10 min, then heated at 160 °C, using the general-purpose bomb by Parr (model 4744), comprising the vessel and cup made of Teflon. Reference sample G was synthesised without the $Ru(NO)(NO_3)_3$ component. After a proper heating time the precipitates were cooled to room temperature (mother liquid pH ≈ 13.5–13.8). The precipitates were separated from the mother liquid using an ultra-speed centrifuge *Sorvall RC2-B*, then subsequently washed with twice-distilled water to remove the »neutral electrolyte«.

Instrumentation

^{57}Fe Mössbauer spectra were recorded at RT in the transmission mode using a standard *WissEl (*Starnberg, Germany) instrumental configuration. The ^{57}Co/Rh Mössbauer source was used. The velocity scale and all data refer to the metallic α-Fe absorber at RT. A quantitative analysis of the recorded spectra was made using the *MossWinn* program.

Fourier transform infrared (FT-IR) spectra were recorded at RT using a *Perkin-Elmer* spectrometer (model 2000).

TABLE II. Phase composition of the samples, as found by X-ray powder diffraction

Sample	r = [Ru] / ([Ru] + [Fe])	Autoclaving time / hours	Phase composition by XRD
G	0	2	α-FeOOH
G1	0	72	α-FeOOH
R1	1.0×10^{-4}	72	α-FeOOH + α-Fe_2O_3
R2	2.5×10^{-4}	24	α-FeOOH + Fe_3O_4 + α-Fe_2O_3
R3	1.0×10^{-3}	24	Fe_3O_4
R4	2.5×10^{-3}	2	α-FeOOH
R5	2.5×10^{-3}	24	Fe_3O_4
R6	5.0×10^{-3}	2	α-FeOOH
R7	5.0×10^{-3}	24	Fe_3O_4

The FT-IR spectrometer was linked to a PC with an installed IRDM (IR Data Manager) program to process the recorded spectra. The specimens were pressed into small discs using a spectroscopically pure KBr matrix.

X-ray powder diffractometer APD 2000 (Cu $K\alpha$ radiation, graphite monochromator, NaI-Tl detector) manufactured by *ItalStructures* (Riva Del Garda, Italy) was used.

A thermal field emission scanning electron microscope (FE-SEM, model JSM-7000F, manufactured by *JEOL Ltd.*) was used. FE-SEM was linked to the EDS/INCA 350 (energy dispersive X-ray analyser) manufactured by *Oxford Instruments Ltd*. The specimens were not coated with an electrically conductive surface layer.

RESULTS AND DISCUSSION

X-ray Powder Diffraction

The results of XRD phase analysis are given in Table II, whereas selected XRD patterns are shown in Figures 1 and 2. Crystal phases were determined from XRD patterns using JCPDS PDF cards No. 29–713 for α-FeOOH, No. 13–534 for α-Fe_2O_3 and No. 19–629 for Fe_3O_4.[22]

α-FeOOH was obtained as a single phase by hydrothermal heating at 160 °C for 2 h (sample G) and 72 h (sample G1) of the suspensions without ruthenium ions. However, we have found that the adding of small amounts of ruthenium in the form of $Ru(NO)(NO_3)_3$ had a drastic effect on that precipitation process. $Ru(NO)(NO_3)_3$ was chosen as a very convenient ruthenium salt which does not undergo hydrolysis in the solid state and dissolves into a transparent solution. On the other hand, ageing of the ruthenium salt $RuCl_3 \cdot xH_2O$ for a prolonged time results in oxidation and the formation of a Ru(IV)-(hydrous)oxide. At the concentration ratio $r = 1.0\times10^{-4}$ (sample R1), where r = [Ru] / ([Ru] + [Fe]), a significant change in the precipitation system was observed upon 72 h of autoclaving. A mixture of α-FeOOH + α-Fe_2O_3 was obtained. With an increase in the ruthenium concentration to obtain $r = 2.5\times10^{-4}$ (sample R2) the phase composition of the precipitate showed the presence of α-FeOOH, Fe_3O_4 and α-Fe_2O_3 (24 h of autoclaving). With a further increase in r to 1×10^{-3}, Fe_3O_4 was detected as a single phase in the precipitate (sample R3). The same

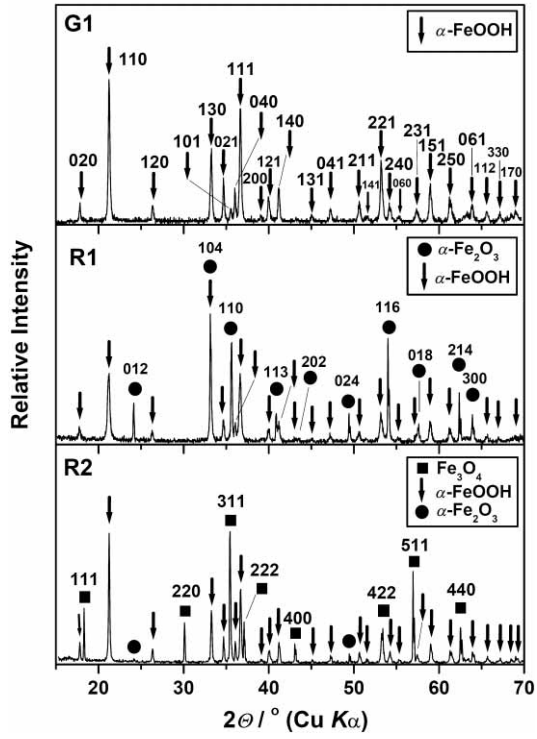

Figure 1. XRD patterns of samples G1, R1 and R2, recorded at RT.

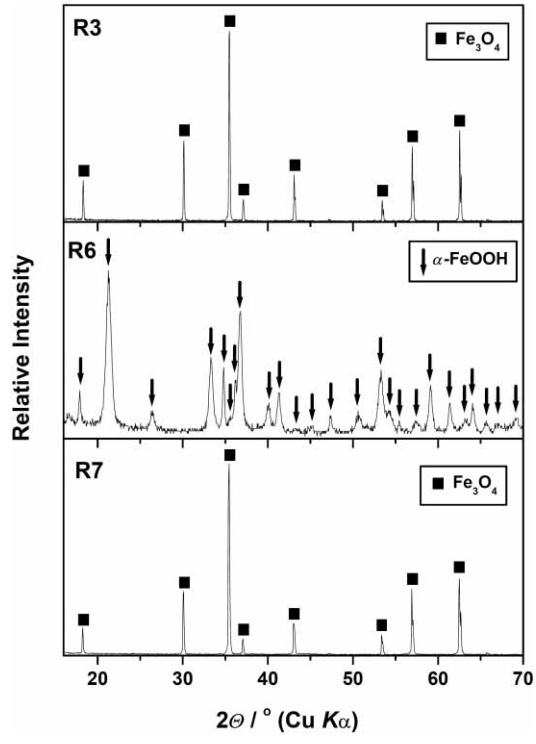

Figure 2. XRD patterns of samples R3, R6 and R7, recorded at RT.

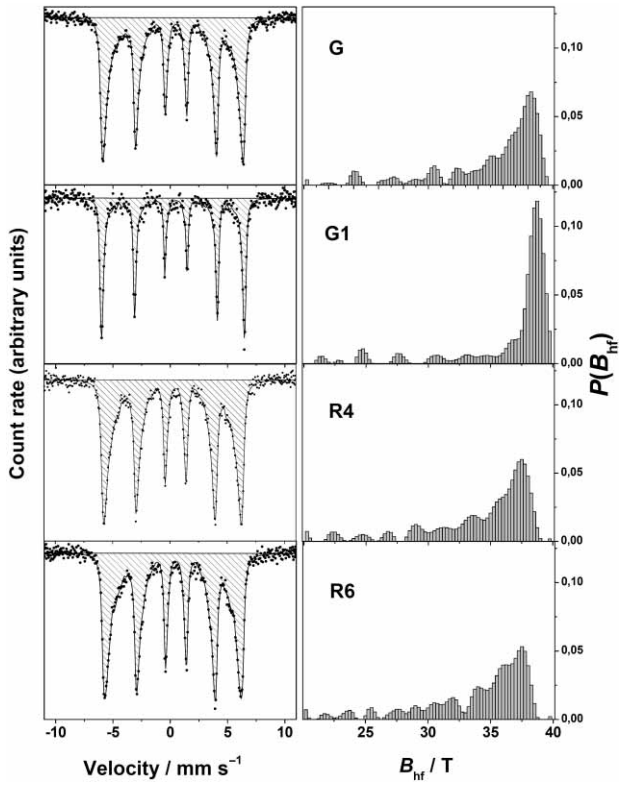

Figure 3. ^{57}Fe Mössbauer spectra of samples G, G1, R4 and R6, recorded at RT.

phase composition was found for samples formed after 24 h of autoclaving in the presence of a higher ruthenium concentration (samples R5 and R7). Samples formed after 2 h of autoclaving (R4 and R6) showed only the lines characteristic of α-FeOOH. XRD analysis of the precipitates showed a very strong effect of the small amounts of ruthenium ions, initially added as a $Ru(NO)^{3+}$ complex. The presence of ruthenium created reductive conditions in the precipitation system, and as a result Fe_3O_4 could precipitate as a single Fe-bearing phase.

^{57}Fe Mössbauer Spectroscopy

The results of Mössbauer spectroscopic measurements are summarized in Figures 3 and 4, whereas the calculated Mössbauer parameters are given in Table III. Mössbauer spectra of samples G, G1, R4 and R6 correspond to α-FeOOH (Figure 3). These spectra show a sextet with broadened spectral lines which deviate from the theoretical intensity ratio 3:2:1:1:2:3. The spectrum of sample G1 displays noticeably better shaping due to increased crystallinity at a prolonged autoclaving time. The RT Mössbauer spectrum of α-FeOOH may vary from one paramagnetic doublet up to a well-shaped sextet, which depends on the size and crystallinity of α-FeOOH particles. α-FeOOH particles smaller than $\approx$ 15–20 nm show a superparamagnetic type of the Mössbauer spectrum at RT, whereas α-FeOOH particles smaller than 8 nm show a superparamagnetic type of the Möss-

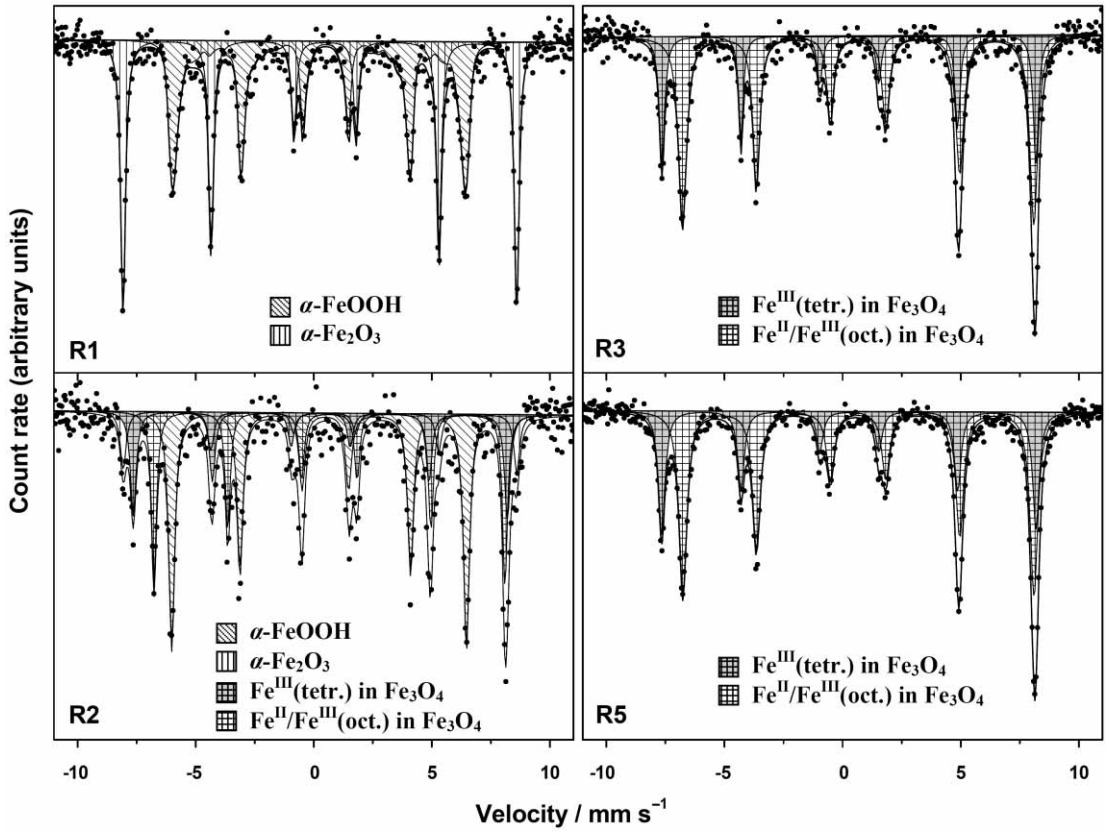

Figure 4. ^{57}Fe Mössbauer spectra of samples R1, R2, R3 and R5, recorded at RT.

TABLE III. ^{57}Fe Mössbauer parameters calculated for samples G, G1 and R1 to R7 and identification

Sample	Spectral line	$\delta^{(a),(b)}$ / mm s^{-1}	$E_q^{(b)}$ / mm s^{-1}	$B_{hf}^{(b)}$ / T		$B_{hf}^{(b)}$ / T	Γ / mm s^{-1}	Area / %	Identification
				average	most probable				
G	M	0.37	–0.26	35.3	38.2		0.28	100	α-FeOOH
G1	M	0.37	–0.26	36.7	38.7		0.20	100	α-FeOOH
R1	M_1	0.37	–0.28	36.1	38.5		0.22	50.8	α-FeOOH
	M_2	0.37	–0.22			51.7	0.25	49.2	α-Fe_2O_3
R2	M_1	0.36	–0.26			38.7	0.31	43.3	α-FeOOH
	M_2	0.37	–0.20			51.7	0.29	10.7	α-Fe_2O_3
	M_3	0.29	–0.02			49.1	0.25	18.5	Fe^{III}(tetr.) in Fe_3O_4
	M_4	0.67	0.01			46.1	0.30	27.5	Fe^{II}/Fe^{III}(oct.) in Fe_3O_4
R3	M_1	0.28	–0.02			49.1	0.27	31.0	Fe^{III}(tetr.) in Fe_3O_4
	M_2	0.66	0.01			46.1	0.40	69.0	Fe^{II}/Fe^{III}(oct.) in Fe_3O_4
R4	M	0.37	–0.26	34.3	37.5		0.29	100	α-FeOOH
R5	M_1	0.28	–0.02			49.1	0.33	34.9	Fe^{III}(tetr.) in Fe_3O_4
	M_2	0.66	0.02			46.1	0.39	65.1	Fe^{II}/Fe^{III}(oct.) in Fe_3O_4
R6	M	0.37	–0.26	33.9	37.5		0.27	100	α-FeOOH
R7	M_1	0.27	–0.02			49.2	0.39	33.6	Fe^{III}(tetr.) in Fe_3O_4
	M_2	0.67	0.01			46.1	0.48	66.4	Fe^{II}/Fe^{III}(oct.) in Fe_3O_4

(a) Isomer shift (δ) is given relative to α-Fe.
(b) Errors: $\delta = \pm 0.01$ mm s^{-1}, $E_q = \pm 0.01$ mm s^{-1}, $B_{hf} = \pm 0.2$ T.

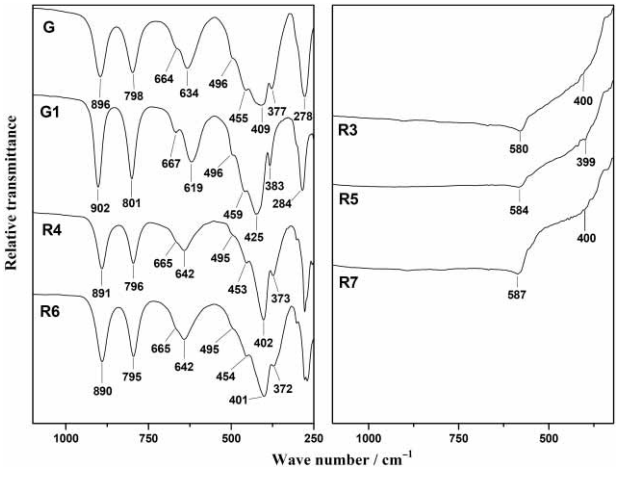

Figure 5. FT-IR spectra of samples G, G1 and R3 to R7, recorded at RT.

bauer spectrum down to 77 K.[23] The goethite sextets in the spectra of samples G, G1, R1, R4 and R6 were fitted taking into account the distribution of hyperfine magnetic field (HMF) in the range from 20 to 40 T with a step of 0.25 T. Sample G1 (Figure 3) showed the narrowest distribution of HMF and a ratio of the relative intensities of spectral lines not far from the theoretical one, 3:2:1:1:2:3. Mössbauer spectra of α-FeOOH samples obtained in the presence of ruthenium ions (samples R4 and R6) showed the broadening of spectral lines and the HMF distribution as well as a decrease in average and most probably hyperfine magnetic field (B_{hf}) (Table III). The origin of this reduction in B_{hf} is the incorporation of ruthenium ions into the α-FeOOH crystal structure. Adding very small amounts of ruthenium ions, as a $Ru(NO)^{3+}$ complex, to the precipitation system caused a great change in the phase composition of the precipitates formed after longer ageing periods (Figure 4). The calculated Mössbauer parameters and fraction percentages of these phases are given in Table III. Phase analysis of samples R3 to R7 by Mössbauer spectroscopy confirmed the results obtained by XRD. Mössbauer spectra of samples R3, R5 and R7 showed the formation of stoichiometric magnetite (Fe_3O_4). In an earlier work[21] we have also observed the formation of stoichiometric magnetite by autoclaving for 24 h at 160 °C the suspensions with initial r between 2.91×10^{-2} and 9.09×10^{-2}. The Mössbauer parameters calculated for magnetite obtained in the present work corresponded to those reported by Murad and Johnston.[23]

FT-IR spectroscopy

Figure 5 shows the FT-IR spectra of samples G, G1, R4 and R6 (left side) and R3, R5 and R7 (right side). FT-IR spectra of samples G, G1, R4 and R6 correspond to the α-FeOOH crystal structure. Sample G shows two IR bands at 896 and

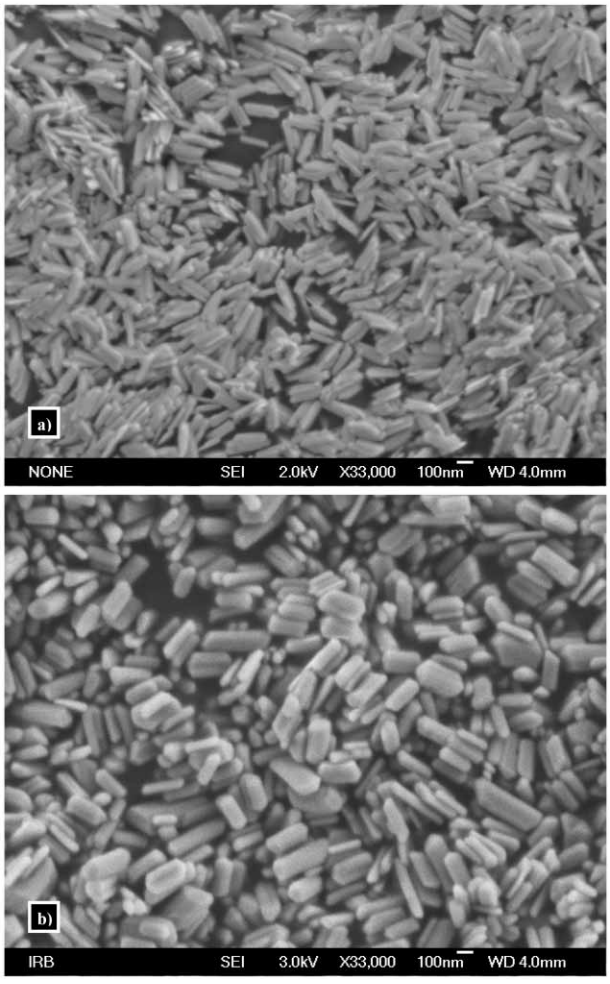

Figure 6. FE-SEM micrographs of samples: (a) G, (b) G1.

798 cm^{-1} which can be assigned to Fe-O-H bending vibrations in α-FeOOH. These bands are usually used for the identification of α-FeOOH in a qualitative phase analysis of *iron oxide* mixtures. The IR band at 634 cm^{-1} with a shoulder at 664 cm^{-1}, very strong and broad IR bands at 409 cm^{-1} with a shoulder at 496 cm^{-1}, and small intensity IR bands at 455 and 377 cm^{-1} were present in the spectrum of sample G. Verdonck *et al.*[24] studied the IR spectrum of α-FeOOH using the normal coordinate analysis, and compared the results with the experimental spectra of α-FeOOH and α-FeOOD. The IR bands recorded at 630, 495 and 270 cm^{-1} were rather insensitive to deuteration, so the authors concluded that these IR bands were due to Fe-O stretching vibrations in α-FeOOH. A similar interpretation of IR bands below 650 cm^{-1} was given by Cambier,[25] who also reported that an intense IR band around 630 cm^{-1} was influenced by the shape of α-FeOOH particles. Weckler and Lutz[26] also investigated the IR spectrum of α-FeOOH.

Main spectral features of samples G and G1 were the same; in the spectra of these two samples, however, there were shifts of IR bands. The most pronounced shifts from sample G to sample G1 were 634 $\rightarrow$ 619 cm^{-1} (a lattice band with the transition moment parallel to the *a*-axis) and 409 to 425 cm^{-1} (a lattice band with the transition moment parallel to the *c*-axis). The shoulder at 664 cm^{-1} for sample G changed to a band of weak intensity at 667 cm^{-1} for sample G1 and the weak band at 377 cm^{-1} for sample G was better pronounced at 383 cm^{-1} for sample G1. The IR band at 425 cm^{-1} (sample G1) was also less broadened. These differences can be assigned to a better crystallinity of α-FeOOH particles in sample G1 than in sample G, an increase in particle thickness (the *a*-axis direction) and a decrease in their shape anisotropy at a longer ageing time.

α-FeOOH particles precipitated in the presence of ruthenium ions (samples R4 and R6) showed lattice vibration bands at 642 and 402 cm^{-1} for sample R4, and 642 and 401 cm^{-1} for sample R6. The shifts in the positions of those bands, in comparison with the bands in the spectrum of sample G, can be assigned to the formation of solid solutions α-(Fe,Ru)OOH and to an elongation of particles in the *c*-axis direction. Moreover, the positions of OH bending bands at 891 and 796 cm^{-1} for sample R4 and 890 and 795 cm^{-1} for sample R6 were slightly different from those recorded for sample G (896 and 798 cm^{-1}). These results show that the most influenced IR bands in α-FeOOH doped with ruthenium ions are those related to Fe-O stretching (lattice) vibrations, thus confirming the incorporation of ruthenium ions in the α-FeOOH structure. It can be concluded that a lower degree of crystallinity of α-FeOOH and Ru substitution in α-FeOOH had a similar effect on the corresponding IR spectrum.

FT-IR spectra of samples R3, R5 and R7 showed an IR band centred between 580 and 587 cm^{-1} and a very broad shoulder (band) at $\approx$400 cm^{-1}. These spectra are consistent with the spectrum of magnetite quoted in literature.[27]

FE-SEM

Figure 6 shows the FE-SEM micrographs of the particles in samples G and G1 which correspond to α-FeOOH. Acicular and uniform α-FeOOH particles (Figure 6a) were obtained by autoclaving of the starting suspension for 2 h at 160 °C. With a heating time prolonged up to 72 h these particles did not much increase in length (Figure 6b). However, within that time a lateral aggregation of α-FeOOH rods was observed, and as a result the width of α-FeOOH particles increased. Electron microscope inspection showed that the crystal growth of bigger (secondary) α-FeOOH particles was governed by a lateral aggregation of primary α-FeOOH rods.

Figure 7a shows rod-like α-FeOOH particles deposited on much bigger α-Fe_2O_3 particles (sample R1). The HMF value of 51.7 T was measured by Mössbauer spectroscopy for the α-Fe_2O_3 fraction in sample R1. This HMF value is typically obtained for large and well-crystallized α-Fe_2O_3 particles. It can be inferred that these α-Fe_2O_3 particles did not show a tendency to form α-$(Fe,Ru)_2O_3$ solid solutions. Figure 7b shows a great population of small α-FeOOH rods and a large Fe_3O_4 (or α-Fe_2O_3) particle (sample R2). Figure 7c shows α-(Fe,Ru)OOH particles (sample R4) elongated along the crystallographic *c*-axis. These particles were grown during the autoclaving of the initial suspension ($r = 2.5 \times 10^{-3}$) for 2 h at 160 °C. The formation of μm size Fe_3O_4 particles

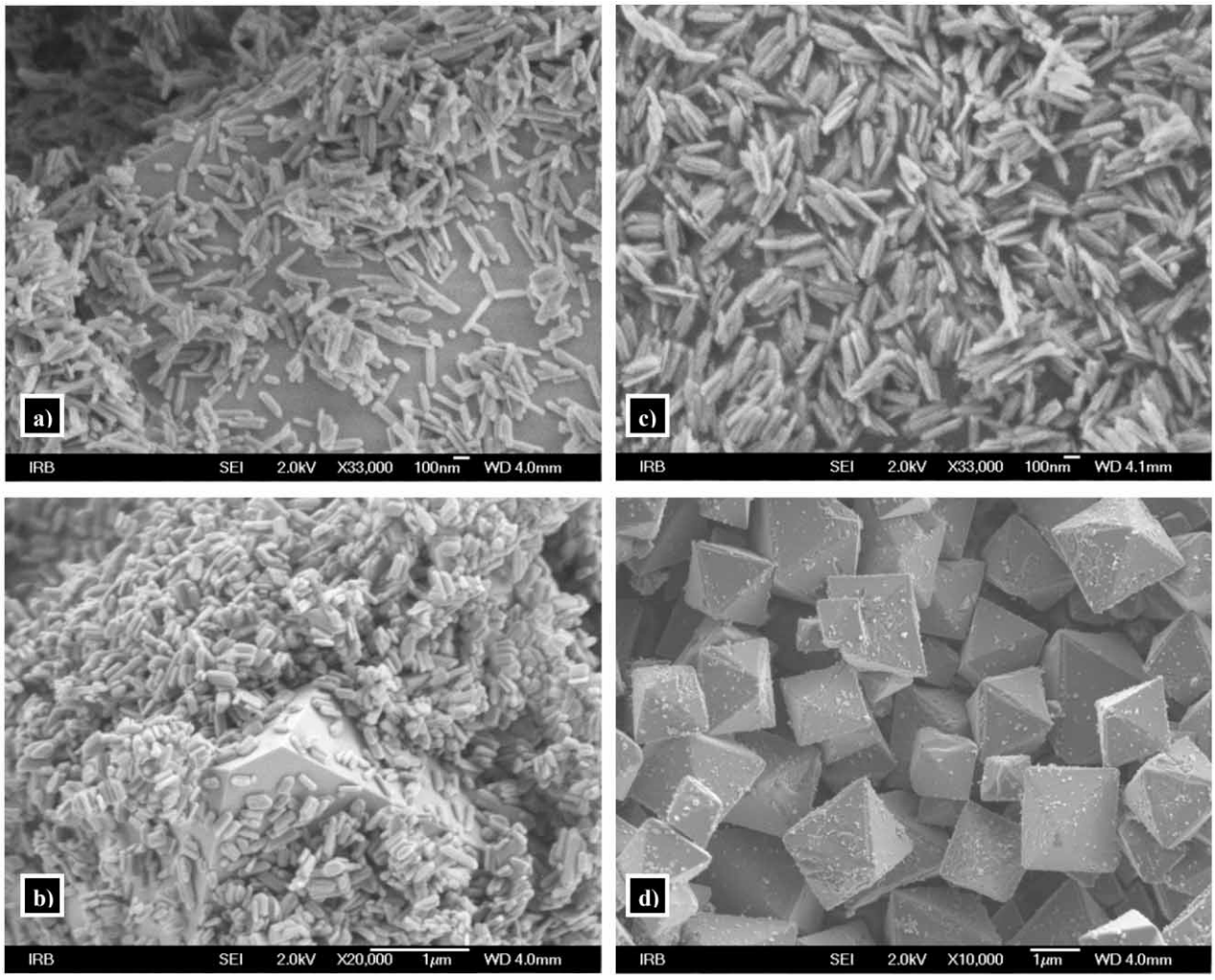

Figure 7. FE-SEM micrographs of samples: (a) R1, (b) R2, (c) R4, (d) R5.

with characteristic octahedral shape was observed upon a prolonged heating time (24 h) at 160 °C (Figure 7d; sample R5).

Figure 8a shows α-(Fe,Ru)OOH particles in sample R6. These particles are elongated along the crystallographic *c*-axis, and the decreased HMF value indicates the incorporation of ruthenium ions into the α-FeOOH crystal structure. The formation of μm range Fe_3O_4 particles was observed upon a prolonged heating time (24 h) at 160 °C (Figure 8b). Figure 8c shows one plane of a Fe_3O_4 crystal at high optical magnification, covered with nanosize particles some of which are aggregated. With an aim to obtain more data about these particles we analysed them by EDS. Generally, the population of these small particles increased in the precipitation systems with an increase in the starting $Ru(NO)(NO_3)_3$ concentration. Figures 9a,c show the FE-SEM micrograph of sample R3 ($r = 1.0 \times 10^{-3}$) precipitated for 24 h at 160 °C. Two selected areas were analysed by EDS. One (Figure 9a) represents a part of one plane of the Fe_3O_4 crystal which was not covered with small particles (light spots). EDS analysis of this selected area showed only iron and oxygen. EDS analysis of the other one (Figure 9c) within a cluster of small particles (light spots) showed a significant amount of ruthenium (Figure 9d). FE-SEM of this cluster under high optical magnification showed both ruthenium particles and small Fe_3O_4 particles. The size of these Fe_3O_4 particles was ≈ 100 nm or less. EDS results are consistent with Mössbauer measurements which did not prove the incorporation of ruthenium in ionic state into the Fe_3O_4 crystal structure.

Effect of Ruthenium Ions on the Precipitation Mechanism

The present work has indicated a complex mechanism of the precipitation of *iron oxides* in the presence of ruthenium. A reference sample of α-FeOOH was obtained using the procedure described in our previous work.[28] Under the precipitation conditions utilised in that work as well as in this one, very high pH values ≈ 13.5–13.8 can be obtained using TMAH as a precipitating agent. In the case of TMAH application the initially formed precipitate (ferrihydrite) can be dissolved on strong shaking, as observed by the naked eye. α-FeOOH is formed after some ageing time under homogenous precipitation conditions. Due to that, by autoclaving of the precipitation system at 160 °C it was possible to obtain

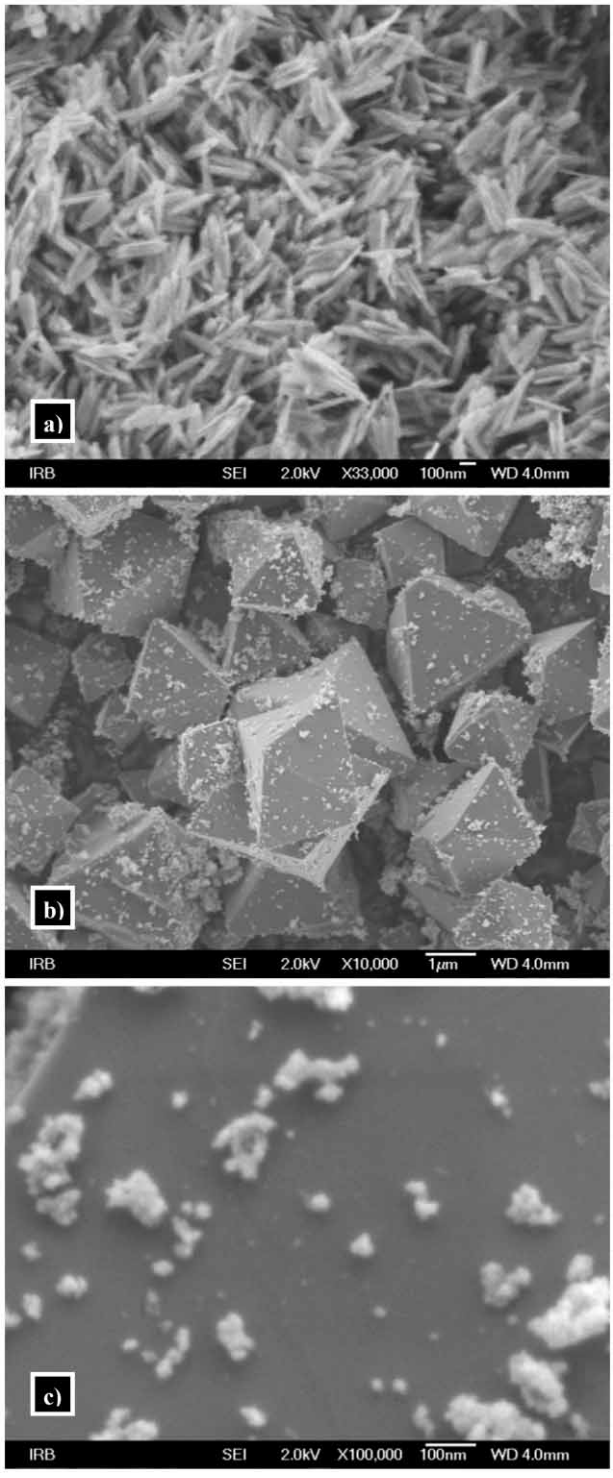

Figure 8. FE-SEM micrographs of samples: (a) R6, (b) R7 at lower optical magnification, and (c) R7 at higher optical magnification of one plane of the Fe_3O_4 particle.

acicular α-FeOOH particles with narrow size distribution. Thus obtained α-FeOOH particles were structurally very stable and did not transform into other *iron oxides* in the corresponding suspensions.

The addition of a very small amount of ruthenium in the form of a $Ru(NO)^{3+}$ complex to the starting solution (before adding the TMAH solution) had a drastic effect on the precipitation systems investigated in the present work. At the beginning of the precipitation process ruthenium ions were incorporated into ferrihydrite substituting Fe^{3+} ions, or as a co-gel (ferrihydrite + ruthenium (hydrous)oxide). Substitution of ruthenium for Fe^{3+} ions was possible due to similarities in the ionic radii of Fe^{3+} (0.645 Å) and Ru^{4+} (0.62 Å).[29] Crystallization of α-FeOOH as a single phase was observed for shorter times (2h in the present work), whereas the incorporation of ruthenium ions into the α-FeOOH structure was proved by Mössbauer spectroscopy. The incorporation of ruthenium ions delayed the crystallization of α-FeOOH, then favoured the crystallization of α-Fe_2O_3. Factors such as the Fe^{3+} concentration in the solution, the incorporation of ruthenium ions into the α-FeOOH crystal structure, as well as different nucleation rates between α-FeOOH and α-Fe_2O_3 were responsible for the formation of α-(Fe,Ru)OOH and α-Fe_2O_3 phases. Upon a prolonged autoclaving time Fe_3O_4 was formed. Under given experimental conditions Fe_3O_4 can be obtained as a single Fe-bearing phase, as shown in the present work. Mössbauer spectroscopy showed the formation of stoichiometric magnetite, thus suggesting reductive conditions created in the precipitation systems (suspensions). In that part of the overall precipitation mechanism the role of ruthenium is dominant, which can be explained by the catalytic action of ruthenium. Generally, ruthenium dioxide, ruthenium black and ruthenium supported on various carriers are well-known catalysts. The role of ruthenium in our precipitation systems can be associated with the behaviour of TMAH, which decomposes at elevated temperatures while yielding a dominant NH_3, volatile amines and CH_3OH. In the presence of the ruthenium catalyst, NH_3 decomposes to N_2 and H_2, whereas CH_3OH decomposes to CO and H_2. In the present experiments it should be the formation of nascent hydrogen which easily reduces Fe^{3+} to Fe^{2+}. In such a way the conditions for the formation of Fe_3O_4 at high pH are created. Mössbauer spectroscopy did not provide evidence of the incorporation of ruthenium ions into the Fe_3O_4 crystal structure.

The effects of ruthenium catalysts were also observed in some other works. For example, the formation of Fe_3O_4/γ-Fe_2O_3 by a reduction of α-Fe_2O_3 was observed during the investigation of the activity of the ruthenium catalyst in a water-gas shift reaction (WGSR).[30] Berry *et al.*[31] used in situ ^{57}Fe Mössbauer spectroscopy to investigate the effects of pre-treatment of titania-supported iron-ruthenium and iron-iridium catalysts in a hydrogen atmosphere. Musić *et al.*[32] used a ruthenium catalyst in the denitration of simulated highly radioactive liquid waste (HRLW) compositions using the formic acid as a reducing agent. Ruthenium was added as the $Ru(NO)(NO_3)_3$ salt or as the so-called soluble $RuO_2 \cdot xH_2O$. The influence of rhodium and palladium on denitration reactions was also investigated. Ruthenium and rhodium were good catalysts for denitration reactions during which they created reductive conditions, so the reduction of Fe^{3+} to Fe^{2+} was observed. Fe^{2+} ions were reoxidised by a careful ad-

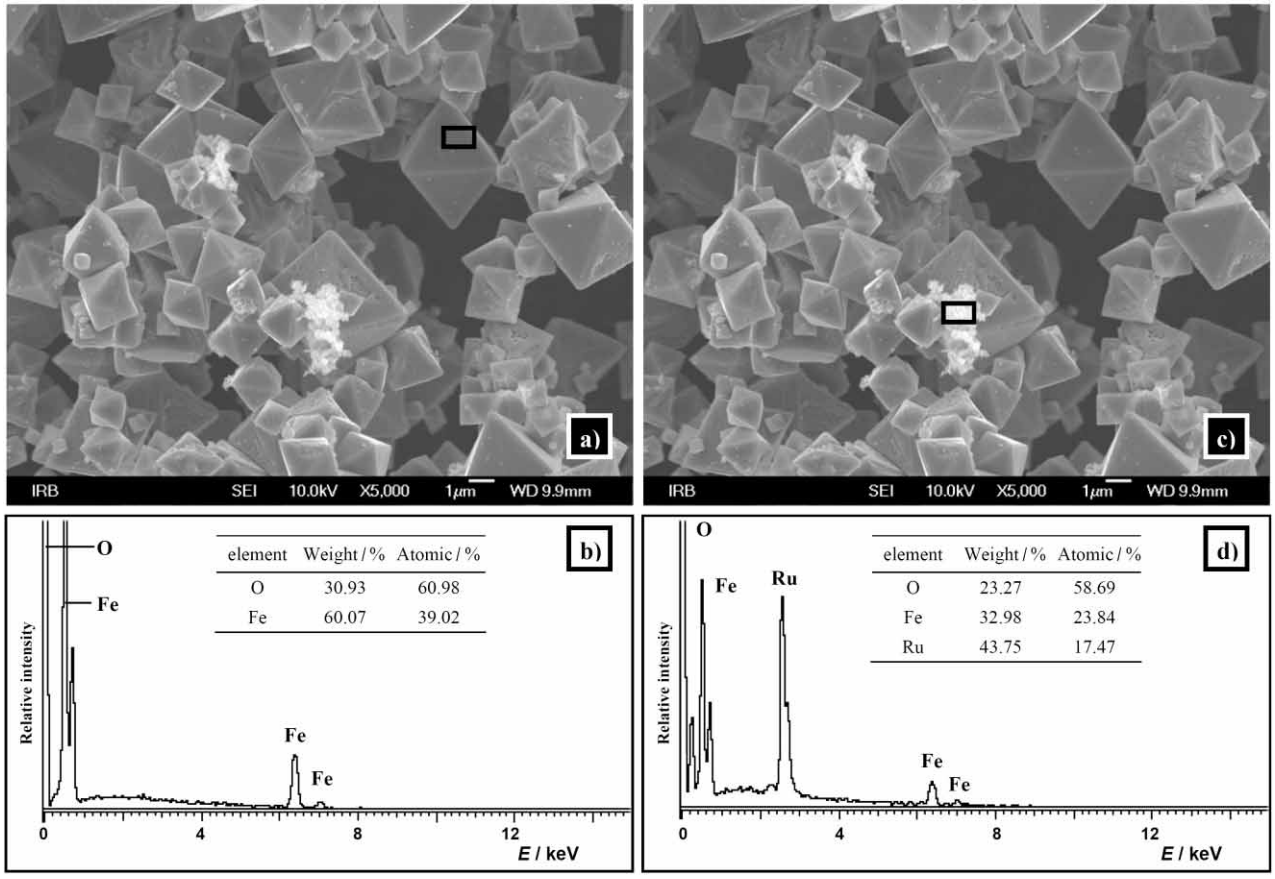

Figure 9. EDS analyses of sample R3.

dition of the concentrated H_2O_2 solution. α-FeOOH and an amorphous fraction were the principal phases in the precipitates upon Fe^{2+} oxidation by H_2O_2.

In the present work the concentrations of ruthenium in the precipitation systems have been very small, so that the ruthenium phase could not be detected with certainty. For that reason we prepared the precipitation system with an increased ruthenium concentration ($r = 3.333 \times 10^{-1}$). XRD of the precipitate formed upon 24 h of autoclaving at 160 °C showed the presence of α-Fe_2O_3 and 2-line ferrihydrite with ruthenium ions incorporated. The presence of metallic ruthenium was not detected by XRD. On the other hand, Fe_3O_4 and metallic ruthenium were detected in the precipitate obtained upon 72 h of autoclaving at 160 °C. Furthermore, the precipitation system ($r = 4.76 \times 10^{-2}$) prepared with NaOH alkali by autoclaving for 24 h did not show the formation of Fe_3O_4. Finally, taking into account these results it can be concluded that the formation of Fe_3O_4 in highly alkaline pH media is a combining effect of the thermal decomposition of TMAH and the catalytic action of ruthenium.

CONCLUSION

• Acicular and uniform α-FeOOH particles were precipitated in line with the procedure described by Krehula *et al.*[28] TMAH was used as a precipitating agent. The phase composition of the α-FeOOH precipitate did not change up to 72 h of autoclaving at 160 °C. The crystal growth of α-FeOOH particles was governed by a lateral aggregation of these particles.

• Adding small amounts of ruthenium in the form of a $Ru(NO)(NO_3)_3$ complex to the starting $FeCl_3$ solution had a drastic effect on the above-mentioned precipitation process at 160 °C. A mixture of α-FeOOH and α-Fe_2O_3 was obtained at an initial concentration ratio $r = 1.0 \times 10^{-4}$ and 72 h of autoclaving. At $r = 2.5 \times 10^{-4}$ and 24 h of autoclaving a mixture of α-FeOOH, Fe_3O_4 and α-Fe_2O_3 was obtained. Fe_3O_4 as a single Fe-bearing phase was obtained at $r = 1.0 \times 10^{-3}$, and higher initial concentrations of $Ru(NO)(NO_3)_3$ after 24 h of autoclaving.

• Addition of ruthenium favoured the formation of stoichiometric Fe_3O_4. The formation of solid solutions was not proved. Mössbauer spectroscopy did not prove the formation of solid solutions between ruthenium and Fe_3O_4 or α-Fe_2O_3, but did prove the formation of α-(Fe,Ru)OOH solid solutions. The phase composition of samples determined by Mössbauer spectroscopy was in line with XRD measurements.

• FT-IR measurements showed that the most influenced IR-bands in the spectra of α-FeOOH particles doped

with ruthenium were those related to Fe-O stretching (lattice) vibrations, thus confirming a conclusion about the incorporation of ruthenium ions into the α-FeOOH crystal structure.

• FE-SEM showed the formation of octahedral Fe_3O_4 particles (crystals) within the μm range size. Ruthenium particles (≈ 20 nm in size) were deposited on the surface of Fe_3O_4 particles. They were also present in the form of clusters. These clusters contained octahedral Fe_3O_4 particles; their size, however, was in the nanosize range (≈ 100 nm or less).

• The formation of Fe_3O_4 was explained by a combining effect of the products of TMAH decomposition and the catalytic activity of ruthenium under autoclaving conditions. This conclusion was supported by additional experiments. By using NaOH instead of TMAH under the same experimental conditions Fe_3O_4 was not formed. It has not been possible to prove with certainty the formation of metallic ruthenium at small concentrations of added $Ru(NO)(NO_3)_3$ and a prolonged autoclaving time. However, at the initial concentrations of $Ru(NO)(NO_3)_3$ much higher than those reported in the present work the formation of metallic ruthenium was confirmed by XRD.

Acknowledgement. – The authors thank to the Ministry of Science, Education and Sport of the Republic of Croatia for financial support (contract no. 0982904-2952).

REFERENCES

1. E. J. W. Verwey and J. H. de Boer, *Recl. Trav. Chim. Pays-Bas* **55** (1936) 531–540.
2. M. E. Fleet, *Acta Crystallogr., Sect. B* **37** (1981) 917–920.
3. M. E. Fleet, *J. Solid State Chem.* **62** (1986) 75–82.
4. S. Musić and S. Popović, *J. Radioanal. Nucl. Chem.* **111** (1987) 27–41.
5. J. García and G. Subías, *J. Phys.: Condens. Matter* **16** (2004) R145–R178.
6. R. S. Hargrove and W. Kündig, *Solid State Commun.* **8** (1970) 303–308.
7. G. Galeczki and A. A. Hirsch, J. *Magn. Magn. Mater.* **7** (1978) 230–233.
8. S. Umemura and S. Iida, *J. Phys. Soc. Jpn.* **47** (1979) 458–467.
9. C. M. Srivastava, S. N. Shringi, and M. V. Babu, *Phys. Status Solidi A* **65** (1981) 731–735.
10. S. J. Harker and R. J Pollard, *Nucl. Instrum. Methods Phys. Res., Sect. B* **76** (1993) 61–63.
11. S. Musić, I. Nowik, M. Ristić, Z. Orehovec, and S. Popović, *Croat. Chem. Acta* **77** (2004) 141–151.
12. S. Musić, Đ. Dragčević, and S. Popović, *Croat. Chem. Acta* **66** (1993) 469–478.
13. T. Ishikawa, H. Nakazaki, A. Yasukawa, K. Kandori, and M. Seto, *Mater. Res. Bull.* **33** (1998) 1609–1619.
14. T. Ishikawa, H. Nakazaki, A. Yasukawa, K. Kandori, and M. Seto, *Corros. Sci.* **41** (1999) 1665–1680.
15. Z. H. Zhou, J. Wang, X. Liu, and H. S. O. Chan, *J. Mater. Chem.* **11** (2001) 1704–1709.
16. T. Ishikawa, Y. Kondo, A. Yasukawa, and K. Kandori, *Corros. Sci.* **40** (1998) 1239–1251.
17. M. Mohapatra, S. Anand, R. P. Das, C. Upadhyay, and H. C. Verma, *Hydrometallurgy* **66** (2002) 125–134.
18. H. Itoh and T. Sugimoto, *J. Colloid Interface Sci.* **265** (2003) 283–295.
19. B. Gržeta, M. Ristić, I. Nowik, and S. Musić, *J. Alloys Compd.* **334** (2002) 304–312.
20. M. Gotić, T. Jurkin, and S. Musić, *Colloid Polym. Sci.* **285** (2007) 793–800.
21. S. Krehula and S. Musić, *J. Alloys Compd.* **416** (2006) 284–290.
22. R. M. Cornell and U. Schwertmann, *The Iron Oxides, Structure, Properties, Reactions, Occurrence and Uses*, Wiley-VCH, Weinheim, Germany, 2003.
23. E. Murad and J. H. Johnston, *Iron Oxides and Oxyhydroxides*, in: G. J. Long (Ed.), *Mössbauer Spectroscopy Applied to Inorganic Chemistry*, Vol. 2, Plenum Publishing Corporation 1987, pp. 507–582.
24. L. Verdonck, S. Hoste, F. F. Roelandt, and G. P. van der Kelen, *J. Mol. Struct.* **79** (1982) 273–279.
25. P. Cambier, *Clay Miner.* **21** (1986) 191–200.
26. B. Weckler and H. D. Lutz, *Eur. J. Solid State Inorg. Chem.* **35** (1998) 531–544.
27. M. S. Ellid, Y. S. Murayed, M. S. Zoto, S. Musić, and S. Popović, *J. Radioanal. Nucl. Chem.* **258** (2003) 299–305.
28. S. Krehula, S. Popović, and S. Musić, *Mater. Lett.* **54** (2002) 108–113.
29. R. D. Shannon, *Acta Crystallogr., Sect. A* **32** (1976) 751–767.
30. A. Basinska, L. Kepinski, and F. Domka, *Appl. Catal., A* **183** (1999) 143–153.
31. F. J. Berry, X. Changhai, and S. Jobson, *J. Chem. Soc., Faraday Trans.* **86** (1990) 165–169.
32. S. Musić, M. Ristić, and S. Popović, *J. Radioanal. Nucl. Chem.* **134** (1989) 353–365.

SAŽETAK

Nastajanje magnetita u jako lužnatom mediju u prisutnosti malih količina rutenija

Stjepko Krehula i Svetozar Musić

Istraživan je utjecaj malih količina rutenija na nastajanje magnetita u jako lužnatom mediju primjenom rentgenske difrakcije u prahu, Mössbauerove spektroskopije, FT-IR spektroskopije, visokorezolucijske pretražne elektronske mikroskopije (FE-SEM) i spektroskopije karakterističnog rentgenskog zračenja (EDS). Izdužene čestice α-FeOOH, pripravljene u jako lužnatom mediju dodatkom tetrametilamonijeva hidroksida (TMAH), korištene su kao referentni materijal. Prisutnost malih količina $Ru(NO)(NO_3)_3$ u taložnom sustavu snažno je utjecala na nastajanje željezovih oksida i njihova svojstva. Dodatak $Ru(NO)(NO_3)_3$ uzrokovao je nastajanje stehiometrijskog Fe_3O_4. S povećanjem početne koncentracije $Ru(NO)(NO_3)_3$ u taložnom je sustavu smanjeno vrijeme potrebno za nastajanje Fe_3O_4 kao jedine faze u talogu koja sadrži željezo. Rutenijevi su ioni ugrađeni u čvrste otopine α-(Fe,Ru)OOH, međutim, nije bilo naznaka o nastajanju čvrstih otopina s α-Fe_2O_3 i Fe_3O_4. Mössbauerova i FT-IR spektroskopija podržale su tvrdnju o nastajanju čvrstih otopina α-(Fe,Ru)OOH. Tehnika FE-SEM pokazala je nastajanje oktaedarskih čestica Fe_3O_4 veličine nekoliko μm. Na površini čestica Fe_3O_4 deponirane su čestice rutenija (veličine $\approx$ 20 nm). Ove čestice su također prisutne u obliku nakupina koje sadrže i oktaedarske čestice Fe_3O_4 veličine $\approx$ 100 nm ili manje. Nastajanje Fe_3O_4 objašnjeno je kombiniranim efektom produkata termičke razgradnje TMAH pri hidrotermičkim uvjetima i katalitičkog djelovanja rutenija, čime se stvaraju jaki redukcijski uvjeti u istraživanom taložnom sustavu.